RNA (2001), *7*:1227–1238. Cambridge University Press. Printed in the USA.

DOI: 10.1017.S1355838201010445

CRS1 is a novel group II intron splicing factor that was derived from a domain of ancient origin

BRADLEY TILL,[1,2] CHRISTIAN SCHMITZ-LINNEWEBER,[1,3] ROSALIND WILLIAMS-CARRIER,[1] and ALICE BARKAN[1]

[1]Institute of Molecular Biology, University of Oregon, Eugene, Oregon 97403, USA

ABSTRACT

Protein-dependent group II intron splicing provides a forum for exploring the roles of proteins in facilitating RNA-catalyzed reactions. The maize nuclear gene *crs1* is required for the splicing of the group II intron in the chloroplast *atpF* gene. Here we report the molecular cloning of the *crs1* gene and an initial biochemical characterization of its gene product. Several observations support the notion that CRS1 is a bona fide group II intron splicing factor. First, CRS1 is found in a ribonucleoprotein complex in the chloroplast, and cofractionation data provide evidence that this complex includes *atpF* intron RNA. Second, CRS1 is highly basic and includes a repeated domain with features suggestive of a novel RNA-binding domain. This domain is related to a conserved free-standing open reading frame of unknown function found in both the eubacteria and archaea. *crs1* is the founding member of a gene family in plants that was derived by duplication and divergence of this primitive gene. In addition to its previously established role in *atpF* intron splicing, new genetic data implicate *crs1* in chloroplast translation. The chloroplast splicing and translation functions of *crs1* may be mediated by the distinct protein products of two *crs1* mRNA forms that result from alternative splicing of the *crs1* pre-mRNA.

Keywords: chloroplast; maize; plastid; RNA chaperone

INTRODUCTION

A variety of biological processes involve highly structured RNA molecules that are found in intimate association with proteins. The contributions of each type of macromolecule to the assembly, structural stability, and functionality of such complexes are not well understood. This is exemplified by group II introns, molecules that have been termed ribozymes because several introns in this class are capable of autocatalytic splicing in vitro (reviewed in Lambowitz et al., 1999). However, self-splicing activity has been observed with only a few group II introns and typically only under high salt conditions. The high salt concentration is believed to aid intron folding, a role that protein cofactors may play in vivo. Genetic data demonstrate that most group II introns do, in fact, require accessory factors to splice efficiently in the cell, but few such factors have been characterized. Genetic screens in maize uncovered two nuclear genes required for the splicing of group II introns in chloroplasts (Jenkins et al., 1997). Mutations in *crs2* disrupt the splicing of many group II introns, all in the IIB subgroup, whereas mutations in *crs1* disrupt the splicing solely of the subgroup IIA intron in the *atpF* gene. Molecular cloning of the *crs2* gene revealed that it encodes a homolog of peptidyl-tRNA hydrolase enzymes (Jenkins & Barkan, 2001). The molecular cloning of the *crs1* gene, described here, indicates that CRS1 is unrelated to CRS2 or to any other protein of known function. However, CRS1 is related to a family of predicted plant proteins and to a conserved open reading frame that is distributed widely in eubacteria and archaea. CRS1 is a highly basic protein that cofractionates with the *atpF* intron under several conditions. These findings provide support for the idea that CRS1 binds in vivo to the *atpF* intron and that it influences splicing via a direct interaction with its intron target. In addition, the properties of a new mutant *crs1* allele suggest that *crs1* is bifunctional, participating in both *atpF* splicing and in the biogenesis or activity of the chloroplast translation machinery.

Reprint requests to: Alice Barkan, Institute of Molecular Biology, University of Oregon, Eugene, Oregon 97403, USA; e-mail: abarkan@molbio.uoregon.edu.

[2]Present address: Fred Hutchinson Cancer Research Center, 1100 Fairview Avenue North, Seattle, Washington 98109-1024, USA.

[3]Present address: Botanisches Institut, Ludwig Maximilians Universitaet Muenchen, Menzinger Str. 67, 80683 Muenchen, Germany.

RESULTS

Molecular cloning of the *crs1* gene

The reference allele of *crs1* (*crs1-m1::MuDR*, hereafter referred to as *crs1-1*) arose in maize lines harboring active *Mutator* (*Mu*) transposons, a high copy number transposon family that is widely used for transposon mutagenesis in maize (Bennetzen, 1996). To identify *Mu* insertions that were genetically linked to *crs1*, DNAs from distantly related mutant seedlings were analyzed by southern hybridization using probes corresponding to each member of the *Mu* family. A *MuDR* probe hybridized to a 4.5-kb *Bgl*II fragment present in all mutant seedlings but absent in closely related homozygous wild-type plants (data not shown). This fragment was cloned by probing a size-selected library of *Bgl*II-digested *crs1-1* DNA with *MuDR* sequences. The position of the *MuDR* insertion in the cloned fragment and the genomic sequence surrounding the insertion are shown in Figure 1. Genomic southern blots probed with sequence flanking this *MuDR* insertion revealed a single *Bgl*II fragment of 4.5 kb in homozygous *crs1-1* samples and a single fragment of 6.2 kb in closely related homozygous wild-type samples (data not shown), showing that the cloned insertion was homozygous in homozygous *crs1-1* mutants.

A second mutant with a *Mu* insertion within the cloned region was identified via a reverse genetic screen. DNA samples from ~1,300 *Mu*-induced nonphotosynthetic mutants were screened by PCR using a primer corresponding to the *Mu* terminal inverted repeat in conjunction with a primer corresponding to the cloned region of the putative *crs1* gene. The mutant recovered, *crs1-2*, had a *Mu1* insertion located 260 bp from the site of the *MuDR* insertion in *crs1-1* (Fig. 1). The splicing defect in *crs1-2* mutants mimics that in *crs1-1* mutants: a failure to splice the *atpF* mRNA but normal splicing of other chloroplast introns (Fig. 2 and data not shown). Furthermore, the two mutations failed to complement when *crs1-1/+* and *crs1-2/+* plants were crossed. That two independent mutant *crs1* alleles have *Mu* insertions within the cloned region provides strong evidence that the cloned insertions disrupt *crs1* function.

Sequences flanking the *MuDR* insertion in *crs1-1* (clone A in Fig. 1A) were used to screen a maize seedling leaf cDNA library, yielding a cDNA clone of 1.8 kb. RNA gel blots probed with this cDNA detected a 2.5-kb RNA in wild-type samples that was undetectable in *crs1-1* and *crs1-2* mutants (Fig. 3A). A cDNA segment representing the 5′ region of the mRNA was obtained

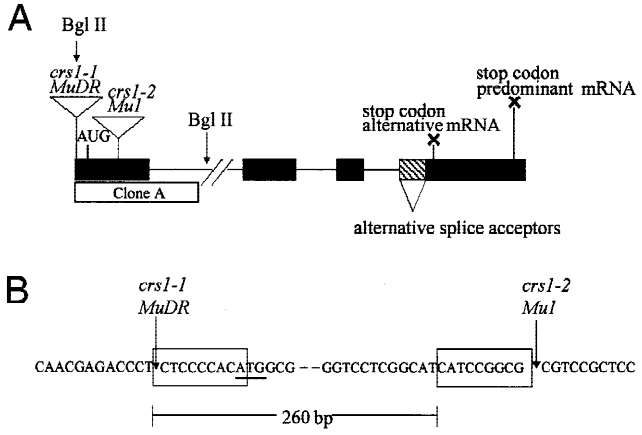

FIGURE 1. Organization of the *crs1* gene. **A:** Map of the *crs1* coding region. Black boxes and thin lines represent exons and introns, respectively. The cross-hatched box represents sequences present as exon in a minor, alternatively spliced mRNA form. The putative start codon and locations of the *Mu* insertions in the two mutant alleles are indicated. The first in-frame stop codons in the predominant and alternatively spliced mRNAs are shown, as are the *Bgl*II sites defining the cloned 4.5-kb genomic fragment of the *crs1-1* allele. Clone A is flanked on one side by the *MuDR* insertion and on the other by the *Bgl*II site. **B:** Genomic sequence surrounding the *Mu* insertions. The *crs1-1* allele contains a *MuDR* insertion 8 bp upstream of the start codon (underlined). The *Mu1* insertion in the *crs1-2* allele maps 260 bp downstream, within the protein-coding portion of exon 1. Boxes outline the target sites that were duplicated upon *Mu* insertion such that they flank the insertions in the mutant alleles. The sequence flanking the *MuDR* insertion exhibited a background-dependent polymorphism: The sequence shown is from the *crs1-1* background; the corresponding sequence in the inbred line B73 lacks 5 bp (5′-TCTCC-3′) in the *MuDR* target site.

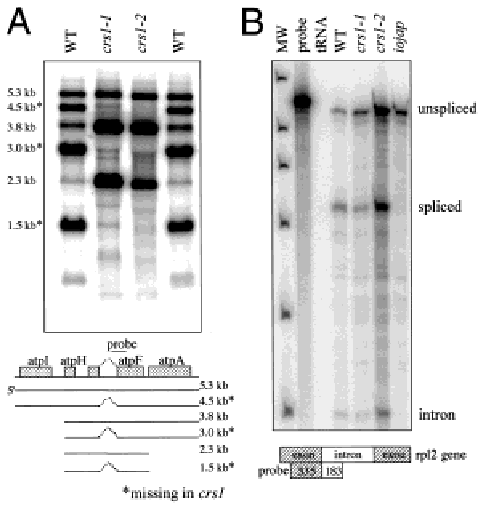

FIGURE 2. *atpF*-specific splicing defect in *crs1-2* mutants. **A:** RNA gel blot illustrating the *atpF* splicing defect in *crs1-2* mutants. Six micrograms of leaf RNA from wild-type (WT), *crs1-1*, or *crs1-2* seedlings was analyzed by hybridization with an *atpF*-specific probe. Beneath the blot, a map of the polycistronic transcription unit containing the *atpF* gene illustrates the structures of the RNAs containing *atpF* sequences (see Jenkins et al., 1997); those marked with asterisks lack the *atpF* intron. **B:** RNAse-protection assay illustrating splicing of the group IIA intron in the chloroplast *rpl2* gene. Five micrograms of leaf RNA were hybridized with the diagramed probe, treated with RNAse T1, and gel fractionated. An albino *iojap* mutant was analyzed to illustrate the *rpl2* splicing defect in mutants that lack plastid ribosomes (Hess et al., 1994; Jenkins et al., 1997). MW: DNA size standards; probe: undigested probe (1/100 of that used in each hybridization); tRNA: tRNA substituted for leaf RNA. The splicing of nine other chloroplast group II introns (*rps12*-introns 1 and 2, *rpl16*, *rps16*, *trnK*, *trnV*, *trnA*, *trnG*, *trnI*) was also examined in *crs1-2* mutants and found to be normal (data not shown).

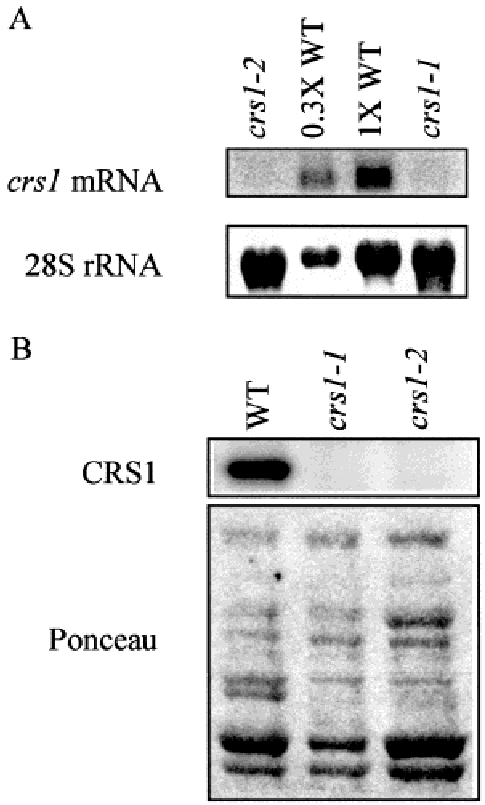

FIGURE 3. Reduced accumulation of *crs1* mRNA and protein in *crs1* mutants. **A:** Thirty micrograms of total leaf RNA, or the indicated dilution, were analyzed by RNA gel blot hybridization, using a *crs1* cDNA probe. An mRNA of 2.5 kb was detected in wild-type (WT) samples but not in mutant samples. The bottom panel shows the abundance of 28S rRNA on the same blot, as visualized by staining with methylene blue. **B:** Chloroplast protein (30 μg) from WT, *crs1-1*, or *crs1-2* seedlings was analyzed by probing an immunoblot with anti-CRS1 antibody. A protein of ~80 kDa was detected in the WT sample, but not in the mutant samples. The bottom panel shows other proteins on the same blot, as visualized by staining with Ponceau S.

by RT-PCR. The full-length cDNA encodes an open reading frame of 715 codons, with the putative start codon mapping 8 bp downstream of the *MuDR* insertion (see Figs. 1 and 4). The predicted product of this mRNA is a protein of 81 kDa. A polyclonal antibody generated against recombinant CRS1 detected a protein of ~80 kDa in wild-type chloroplasts that was not detectable in either *crs1-1* or *crs1-2* mutant chloroplasts (Fig. 3B). The size, immunoreactivity, and *crs1*-dependent expression of this protein indicate that it is the product of the *crs1* mRNA.

CRS1 harbors a repeated domain of ancient origin that is found in a family of predicted plant proteins

The *crs1* gene product is predicted by the Target P algorithm (Emanuelsson et al., 2000) to be targeted to the chloroplast. The mature protein (i.e., lacking the predicted 5-kDa chloroplast transit peptide) has a molecular weight of 77 kDa and is highly basic, with a pI of 9.9. Database searches revealed similarity between CRS1 and predicted proteins from 16 distinct loci in *Arabidopsis.* Figure 4 shows an alignment between CRS1 and the two most similar *Arabidopsis* proteins. These proteins each include three copies of a repeated domain of 10 kDa (bracketed in Fig. 4); a similar domain is found in each additional member of the *Arabidopsis* CRS1 family (data not shown). To illustrate the conserved residues in the domain, the nine examples represented in the three proteins shown in Figure 4 are aligned with one another in Figure 5. Intriguingly, this domain is related to the predicted product of a conserved, free-standing open reading frame of unknown function that is found in both archaea and eubacteria. Representative eubacterial (*Escherichia coli*) and archaeal (*Methanococcus jannaschii*) members of the family are included in the alignment in Figure 5. Homologs are found in all of the major archaeal lineages (data not shown) indicating that this gene was present in the common ancestor of extant archaea and predates the evolution of plants and algae. Thus, it appears that the CRS1 gene family arose by duplication of a primitive gene of unknown function.

Alternative splicing generates two *crs1* mRNA forms

The *crs1* cDNA recovered from the cDNA library differed from that obtained by RT-PCR of leaf mRNA with respect to the position of one 3′ splice junction (diagramed in Fig. 1A). The "alternatively" spliced form retains 95 nt as exon that are removed in the "fully" spliced form. To determine the ratio of these two mRNA forms in various tissues, the region spanning the alternative splice junction was analyzed by RT-PCR (Fig. 6A,B). Both forms of the *crs1* mRNA accumulate in all tissues assayed, with the fully spliced RNA accumulating to higher levels than the alternatively spliced version.

Translation of the alternatively spliced form would yield a truncated protein (43 kDa) due to a shift in the reading frame (see Figs. 1A and 4). To date, only the ~80-kDa CRS1 protein, the product of the fully spliced mRNA, has been detected. It remains possible, however, that the alternative product is synthesized but accumulates below detectable levels. Hereafter, "CRS1" will refer to the ~80-kDa product of the fully spliced mRNA, unless otherwise stated.

Developmental profile of *crs1* mRNA accumulation

The splicing of the chloroplast *atpF* mRNA, CRS1's target, is subject to developmental regulation (Barkan, 1989). The largest proportion of *atpF* RNA is spliced in mature leaf tissue containing chloroplasts or etioplasts;

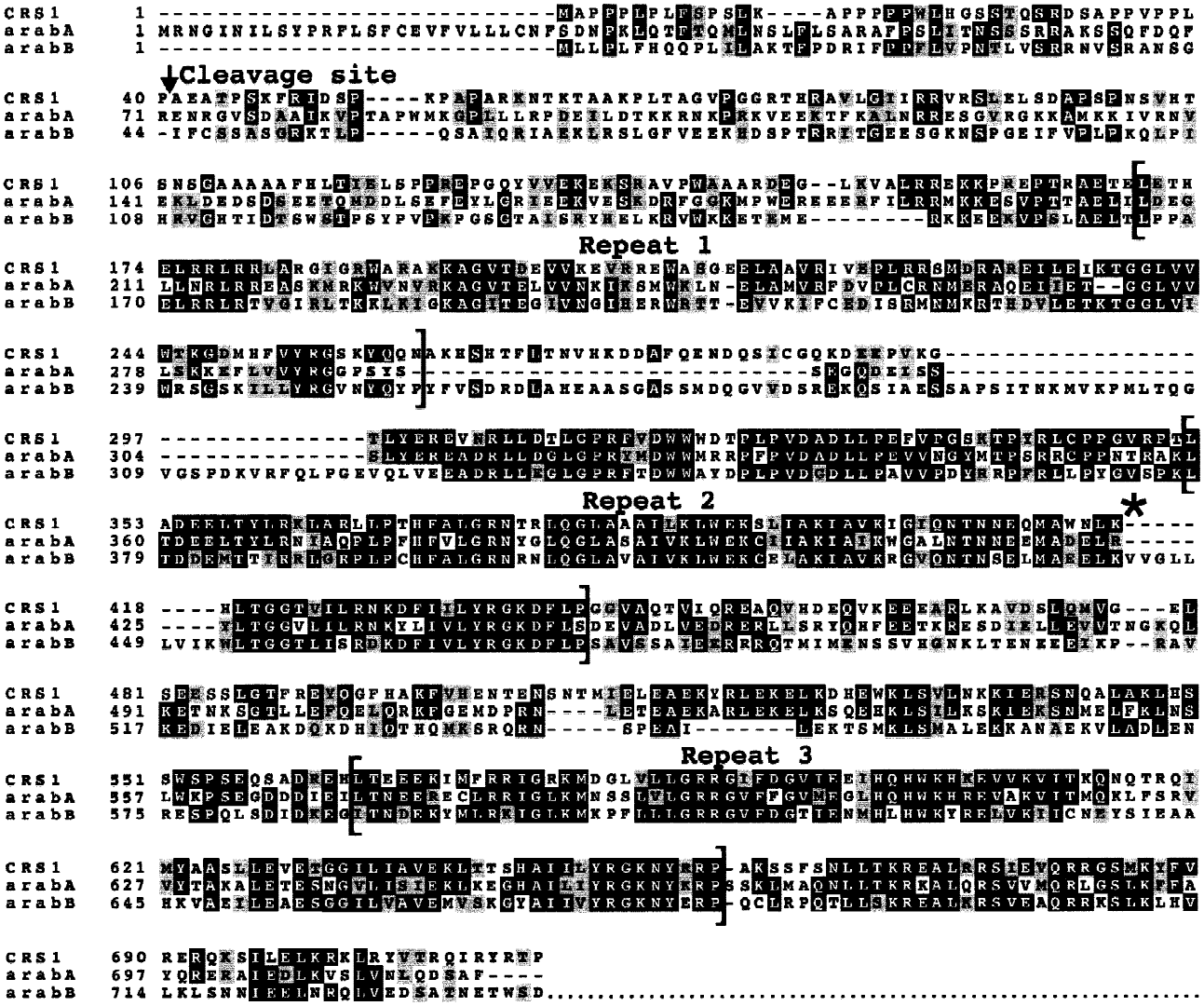

FIGURE 4. Multiple sequence alignment of CRS1 and two *Arabidopsis* homologs. The transit peptide cleavage site predicted for CRS1 (GenBank accession number AAG00595) by the TargetP algorithm (Emanuelsson et al., 2000) is indicated by a vertical arrow. The brackets delineate the three iterations of a degenerate 10 kDa repeated domain. The predicted product of the alternatively spliced *crs1* mRNA (GenBank accession number AF290415) diverges in sequence at the site indicated by the asterisk; 50 additional amino acids (GKAYIGLSLTQSTESVLLLFVFSCVTLKLLSAASYGRHCYIEKQGFYYSI) are encoded by the alternatively spliced mRNA before a stop codon is reached. Arabidopsis A is GenBank accession number CAC01859. Arabidopsis B is GenBank accession number AAF24608, but only the first 740 amino acids of this 1,020 amino acid protein are shown in the alignment.

a lower proportion is spliced in the basal portion of the leaf, which contains proplastids and immature chloroplasts, and a still lower proportion is spliced in root, which contains various nonphotosynthetic plastid forms. To determine whether regulated *crs1* expression might be responsible for these changes in *atpF* splicing, *crs1* mRNA levels were assayed in various tissues. RT-PCR (Fig. 6B) and RNA gel blot (Fig. 6C) assays showed that *crs1* mRNAs accumulate to much higher levels in leaf tip (both green and etiolated) than in roots. These results are consistent with the possibility that a limitation of *crs1* expression in roots contributes to inefficient *atpF* splicing in root plastids. In contrast, *crs1* mRNAs accumulate to a relatively high level in leaf base tissue, suggesting that a factor other than CRS1 limits *atpF* splicing in proplastids. The ratio of fully spliced to alternatively spliced *crs1* mRNA was similar in all tissues examined (Fig. 6B), arguing against the possibility that a switch in the usage of *crs1* splice acceptors is responsible for the activation of *atpF* splicing during leaf development.

Group II introns have been divided into two subgroups, IIA and IIB, based on several subtle structural distinctions (Michel et al., 1989). Maize and barley mutants lacking plastid ribosomes fail to splice all chloroplast introns in subgroup IIA, including the *atpF* intron (Hess et al., 1994; Huebschmann et al., 1996; Jenkins et al., 1997; Vogel et al., 1999). Because the trans-

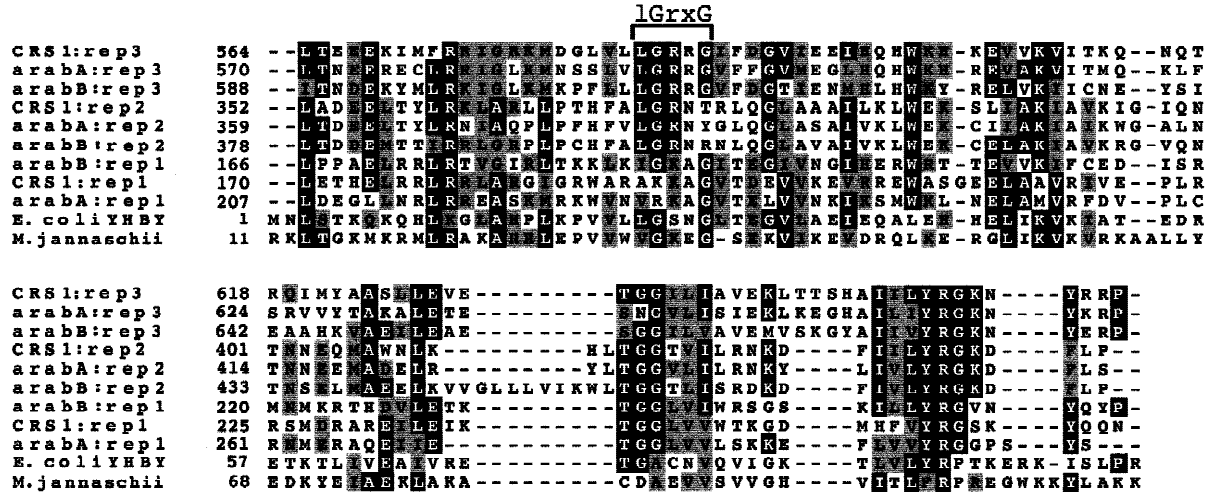

FIGURE 5. Multiple sequence alignment illustrating conserved residues within the repeated domains in CRS1. The alignment includes the nine copies of the repeated domain found in the three proteins aligned in Figure 4, as well as the products of conserved open reading frames in a eubacterium *(E. coli*) and archaea (*M. jannaschii*). Rep1, rep2, and rep3 refer to the first, second, and third copies of the domain in each of the proteins depicted in Figure 4; the residue numbers are shown to facilitate cross-reference. A conserved motif, lGrxG, which resembles a key feature of KH RNA binding domains, is indicated. The entire *E. coli* protein (accession number P42550) is shown. The full *M. jannaschii* protein (accession number Q58068) is 134 amino acids in length, of which amino acids 11–109 are shown.

cription of some nuclear genes encoding chloroplast-localized proteins is repressed in mutants that lack developed chloroplasts (reviewed by Surpin & Chory, 1997), we addressed whether the failure to splice the *atpF* intron in mutants lacking plastid ribosomes might result from the down-regulation of *crs1*. The *crs1* mRNA level in *iojap* mutant leaf tissue lacking plastid ribosomes (Walbot & Coe, 1979) was reduced to a level similar to that in wild-type roots (Fig. 6C). Thus, it is possible that the *atpF* splicing defect in *iojap* mutants results, in part, from the reduction in *crs1* mRNA in leaf cells that lack developed chloroplasts.

CRS1 is found in a ribonucleoprotein complex in the chloroplast stroma that cofractionates with *atpF* intron

To establish the intracellular location of CRS1, its concentration in total leaf extract was compared with that in isolated chloroplasts (Fig. 7A). Mitochondrial and cytosolic markers (MDH and PEPCase, respectively) were depleted in the chloroplast fraction, illustrating its degree of purity. As anticipated by the *crs1* mutant phenotype and the fact that CRS1 has a predicted chloroplast targeting sequence, CRS1 was enriched in the chloroplast fraction to a similar degree as an established chloroplast protein, CRP1 (Fisk et al., 1999). Immunoblots of chloroplast subfractions (Fig. 7B) showed that CRS1 fractionated with CRP1, a stromal marker, and not with markers for the thylakoid (OE33) or envelope (IM35) membranes. Thus, CRS1 is localized to the chloroplast stroma.

To determine whether CRS1 is stably associated with other molecules in vivo, stroma was fractionated by sedimentation through sucrose gradients (Fig. 8). CRS1 sedimented more rapidly than Rubisco (~550 kDa) and more slowly than chloroplast ribosomes, indicating that it is found in a large nonribosomal complex. To investigate the possibility that this complex includes *atpF* intron RNA, RNA was purified from the gradient fractions and analyzed by RNA gel blot hybridization. *atpF* intron RNA cosedimented with CRS1, whereas group II introns that do not require CRS1 for splicing (*petB*, *ndhB*) sedimented more slowly (Fig. 8). The *atpF* intron RNA molecules detected were ~800 nt in length, a size similar to that of the excised intron (833 nt). However, these intron-length molecules may have arisen during extract preparation by degradation of *atpF* pre-mRNA down to a nuclease-resistant intron core. This latter possibility is supported by the fact that intact *atpF* pre-mRNAs were not detected in any gradient fractions (data not shown) despite their high abundance in the chloroplast (see Fig. 2A). In any case, the sedimentation rate of the intron RNA revealed that it is in a particle of >600 kDa, indicating that the intron RNA (~270 kDa) is bound in a multimeric complex.

RNase A treatment of stroma prior to centrifugation reduced the sedimentation rate of the CRS1 complex (Fig. 9A), suggesting the presence of RNA in the complex. However, the reduction in sedimentation rate was less than would be anticipated if the 800 nt *atpF* intron RNA was (1) bound to CRS1 in the native complex and (2) eliminated by the RNase treatment. It seemed plausible, however, that the *atpF* intron resisted complete digestion by the RNase A because it is highly structured or protected by protein, thereby accounting for the small change in CRS1 particle size. In support of this possibility, a peak of RNase A-resistant *atpF* intron

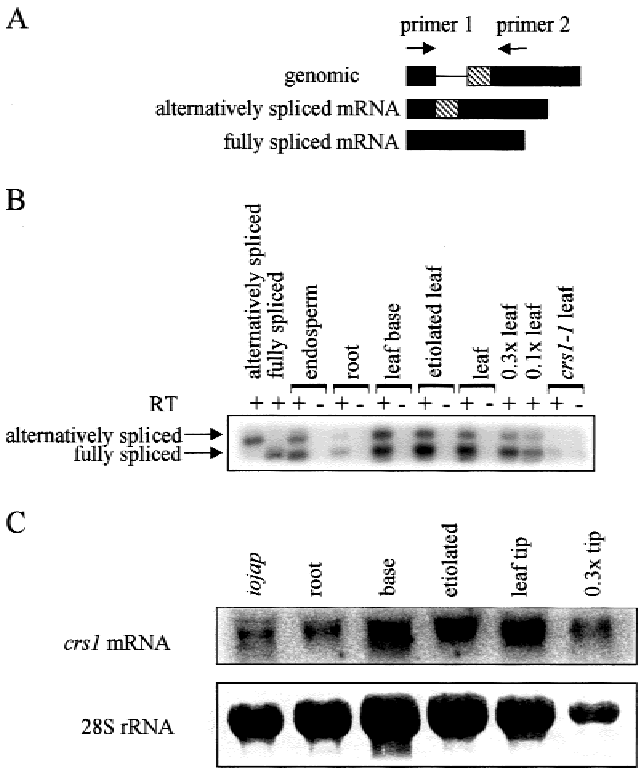

FIGURE 6. Alternative splicing generates two *crs1* mRNA forms. **A:** Map of the genomic region encoding the alternative splice junction. Black boxes and the thin line represent regions present as exon and intron, respectively, in both mRNA forms (see Fig. 1A). The cross-hatched box illustrates the segment found as exon specifically in the alternatively spliced RNA. Primers 1 and 2 were used in the RT-PCR assay shown in **B**. **B:** RT-PCR analysis illustrating the relative abundance of two *crs1* mRNA forms. Reactions contained 10 μg of total RNA from the following tissues: endosperm, seedling root, seedling leaf base, etiolated seedling leaf tip, green seedling leaf tip (leaf), and *crs1-1* leaf. Dilutions of the wild-type leaf RNA sample (0.3× and 0.1×) were analyzed to illustrate the linearity of the assay. The presence (+) or absence (−) of reverse transcriptase in the reaction is indicated above each lane. The first two lanes show the PCR products of cDNAs representing either the alternative or fully spliced mRNA. The PCR products were detected by southern hybridization using a *crs1* cDNA probe. The nucleotide sequences of representative PCR products from this experiment were determined to confirm that they represent the mRNA forms diagramed in **A**. **C:** RNA gel blot showing *crs1* mRNA abundance in different tissues. Thirty micrograms of total RNA (or the indicated dilution) from wild-type seedling root, leaf base (base), etiolated leaf tip (etiolated), or leaf tip were assayed. Thirty micrograms of leaf RNA from an albino *iojap* mutant were assayed to assess *crs1* mRNA accumulation in the absence of chloroplast development. The lower panel shows the abundance of 28S rRNA on the same blot, visualized by staining with methylene blue.

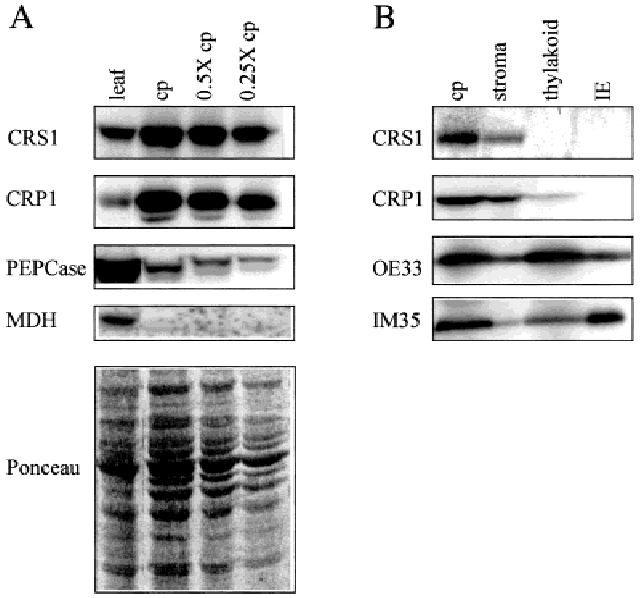

FIGURE 7. Immunoblots of leaf and chloroplast subfractions. **A:** Seedling leaf (leaf) or chloroplast (cp) extract (20 μg protein or the indicated dilutions) were analyzed on an immunoblot by probing sequentially with antisera specific for CRS1, CRP1 (a chloroplast marker), PEPCase (a cytosolic marker), or MDH (a mitochondrial marker). The lower panel shows the results of staining the filter with Ponceau S, to visualize total bound proteins. **B:** Total chloroplast (cp), stromal, thylakoid membrane, or inner envelope (IE) proteins were analyzed on replicate immunoblots by probing with antisera specific for CRS1, CRP1 (a stromal marker), OE33 (a thylakoid marker), or IM35 (an inner envelope marker). Lanes contain protein from an equivalent number of chloroplasts.

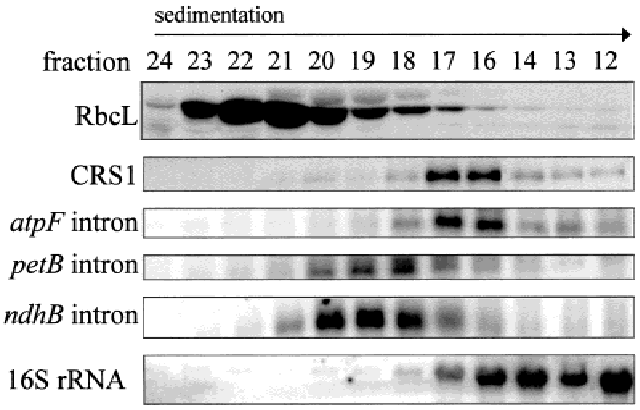

FIGURE 8. CRS1 cosediments with *atpF* intron RNA. Stroma was sedimented through a sucrose gradient and divided into 31 fractions. The top two panels show immunoblots of fractions 12–24, probed with antisera to Rubisco (RbcL) or CRS1. RNA purified from the same fractions was analyzed by RNA gel blot hybridization (bottom four panels), using probes specific for the *atpF* intron, *petB* intron, *ndhB* intron, or 16S rRNA. Fraction 15 contained CRS1 protein but is not shown because the RNA from fraction 15 was lost during RNA extraction; the independent experiment shown in Figure 9 (see "untreated" samples) confirms that *atpF* intron and CRS1 cosediment. The 16S rRNA peaked in fraction 11. The fractions not shown contained insignificant amounts of RbcL, CRS1, *atpF* intron, *petB* intron, or *ndhB* intron. The intron RNAs detected were 700–800 nt in length.

RNA was detected in the gradient of RNase A-treated stroma (Fig. 9B, lower panel, fractions 17–20). These RNase A-resistant intron RNA molecules were only ~200 nt, in contrast to the 800-nt intron molecules detected in untreated stroma (Fig. 9B, upper panel). Importantly, the 200-nt *atpF* intron fragment(s) detected after RNase treatment cosedimented with CRS1 in the same gradient (Fig. 9A,B, lower panels). The cosedimentation of CRS1 and *atpF* intron RNA during centri-

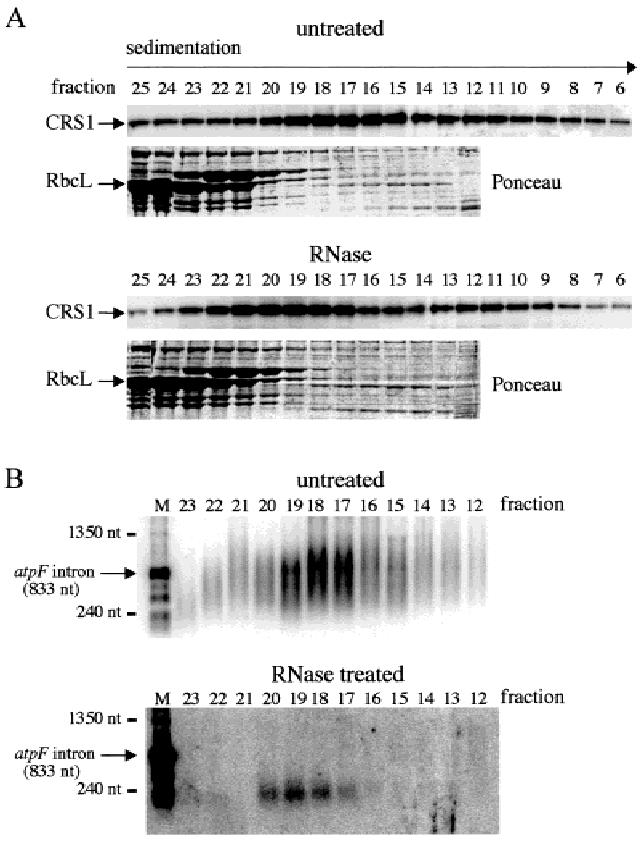

FIGURE 9. RNase A treatment causes a similar decrease in the rate of CRS1 and *atpF* intron sedimentation. Untreated stroma or stroma that had been incubated with RNase A was fractionated by sedimentation through sucrose gradients. The gradients were divided into 35 fractions. **A:** Immunoblots showing distribution of CRS1 in the gradients (upper panels). Only trace amounts of CRS1 were detected in fractions 26–35 and 1–5 (not shown). The lower panels show the results of staining duplicate blots with Ponceau S, with the band corresponding to the large subunit of Rubisco (RbcL) indicated. RNase treatment caused a reduction in the sedimentation rate of the CRS1 particle but not of Rubisco or the other abundant proteins in the extract. The Rubisco peaks also serve as an internal standard to aid comparison of CRS1 sedimentation in Figures 8 and 9. The breadth of the CRS1 peak may reflect heterogeneity in the amount of associated *atpF* RNA that survived extract preparation, or heterogeneity in other factors that associate with CRS1. **B:** RNA gel blots showing distribution of *atpF* intron RNA in the same gradients. The intron RNA in this experiment is more degraded than that shown in Figure 8 because this stromal extract was not treated with RNAse inhibitors, which otherwise would have interfered with the RNAse A treatment. The RNA from fraction 21 of the RNAse A treated extract was lost during extraction, accounting for the lack of signal in that lane. M: denatured PCR fragment corresponding to the *atpF* intron (833 nt) mixed with an RNA size ladder. The positions of the 240-nt and 1,350-nt RNA markers are indicated.

fugation of untreated stroma (Fig. 8 and "untreated" samples in Fig. 9) and their similar reduction in sedimentation rate after RNase A treatment (RNase-treated samples in Fig. 9), together with the genetic data implicating CRS1 in *atpF* splicing, provide strong evidence that CRS1 is found in a stable and specific complex with *atpF* intron RNA in vivo. The size of the CRS1 complex in untreated stroma, at 600–700 kDa, is substantially larger than the sum of the masses of CRS1 (~80 kDa) and *atpF* intron RNA (~270 kDa), suggesting that the complex involves a CRS1 multimer, multiple copies of the RNA, and/or unidentified components.

The *crs1* gene functions in both *atpF* splicing and chloroplast translation

Although the *crs1* mRNA and protein are below detection limits in both *crs1-1* and *crs1-2* mutants (Fig. 3), the mutant phenotypes suggested that *crs1-2* conditions the more complete loss of *crs1* function. *crs1-2* mutants accumulate less leaf chlorophyll than *crs1-1* mutants (data not shown). This stronger phenotype does not appear to be due to the influence of a second mutation because it cosegregated with *crs1-2* through several generations and because the *crs1-1/crs1-2* plants arising from complementation crosses exhibited an intermediate chlorophyll deficiency. The notion that *crs1-2* is the stronger of the two alleles is supported by the positions of the *Mu* insertions: The insertion in *crs1-1* is upstream of the predicted start codon and may not completely disrupt gene expression, whereas the insertion in *crs1-2* disrupts the *crs1* open reading frame (see Fig. 1A).

As shown previously (Jenkins et al., 1997), *crs1-1* mutants exhibit a severe loss of the ATP synthase complex but only a moderate loss of the other major photosynthetic enzyme complexes (PS II, cytochrome b_6f, PS I, and Rubisco; Fig. 10). In contrast, *crs1-2* mutants exhibit a rather severe deficiency in all of these photosynthetic enzyme complexes (Fig. 10). Because each of these complexes includes chloroplast-encoded subunits, these findings raised the possibility that *crs1* may play a general role in chloroplast gene expression. In support of this idea, analysis of chloroplast polysomes showed that two representative chloroplast mRNAs, *rbcL* and *atpB/E*, were associated with fewer ribosomes in *crs1-2* leaf than in wild-type and *crs1-1* leaf (Fig. 11). Therefore, *crs1-2*, the stronger allele, confers a global defect in plastid translation. The reduced accumulation of *rbcL* mRNA in *crs1-2* mutants (Fig. 11) is similar to that observed previously in global chloroplast translation mutants (Barkan, 1993), and is believed to result from destabilization of the *rbcL* mRNA when it is not bound to ribosomes.

Given the established role of CRS1 in the splicing of a group II intron, it seemed plausible that the global translation defect in *crs1-2* mutants results from the failure to splice one or more of the group II introns found in chloroplast tRNA and ribosomal protein genes. However, the splicing of every such intron was assayed in *crs1-2* mutants and was found to be normal (Fig. 2B and data not shown). Taken together, these results suggest that *crs1* is a bifunctional gene that is required for *atpF* splicing and that also influences chloroplast translation.

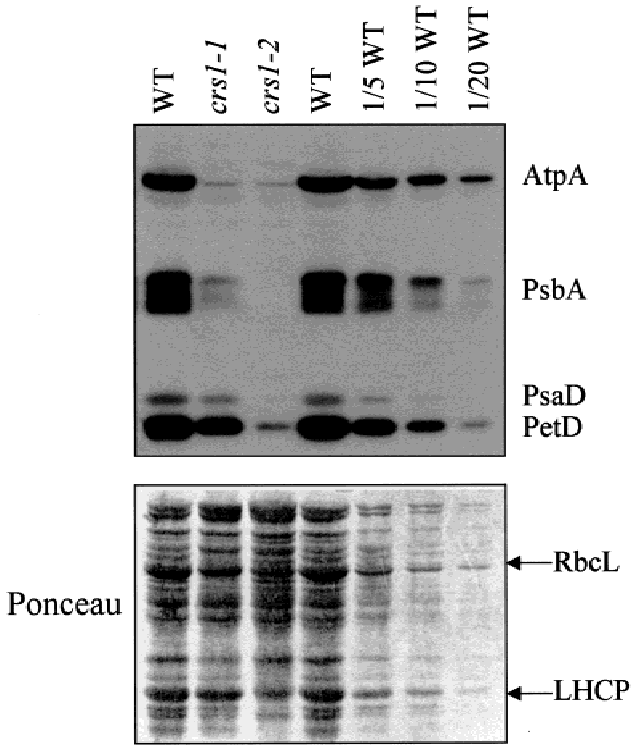

FIGURE 10. Immunoblot showing the abundance of representative subunits of the major photosynthetic complexes in *crs1-1* and *crs1-2* mutants. Five micrograms of leaf protein, or the indicated dilutions of the wild-type (WT) sample, were analyzed. The upper panel shows the results of probing with a cocktail of antisera specific for AtpA (an ATP synthase subunit), PsbA (a PS II subunit), PsaD (a PS I subunit), and PetD (a cytochrome b_6f subunit). The abundance of these subunits generally reflects the abundance of other core subunits in each complex (Barkan et al., 1995). The bottom panel shows the result of staining the same blot with Ponceau S, to visualize total proteins. The stained bands corresponding to RbcL and LHCP (the major chlorophyll *a/b* binding protein) are indicated.

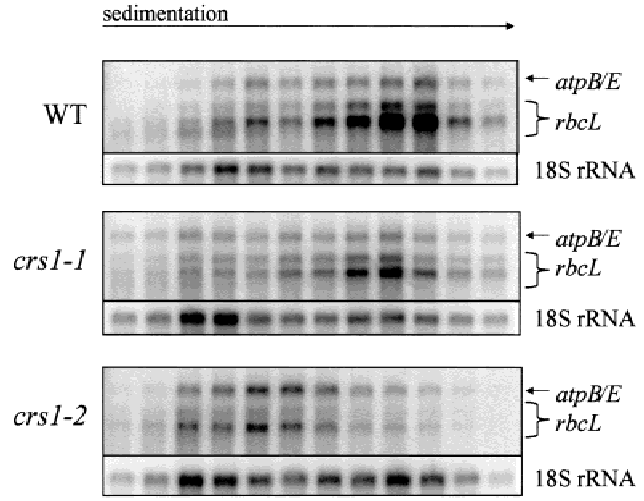

FIGURE 11. Reduced size of chloroplast polysomes in *crs1-2* mutants. Total leaf extracts were sedimented through sucrose gradients under conditions that maintain polysome integrity (Barkan, 1998). 80S ribosomes peaked in the fourth fraction from the top of the gradients (data not shown). Fractions nearer the bottom of the gradients contained polysomes of increasing size. RNA purified from gradient fractions was analyzed on RNA gel blots by hybridization with a probe that detects the chloroplast *atpB/E* and *rbcL* mRNAs. The blots were reprobed with an 18S rRNA probe, revealing the distribution of cytosolic 40S ribosomal subunits and illustrating the integrity of cytosolic polysomes in the same extracts.

DISCUSSION

Few group II intron splicing factors have previously been described at the molecular level. The results presented here add to this data set by providing a description of CRS1, a maize protein required for the splicing of a single group II intron in the chloroplast. The *crs1* gene is a member of a predicted gene family in plants, and encodes a basic, chloroplast-localized protein. Cosedimentation of CRS1 and *atpF* intron RNA during sedimentation of stroma through sucrose gradients, and their similar reduction in sedimentation rate after RNase treatment, suggest that CRS1 is bound in a stable fashion to its target intron in vivo. Thus, the splicing defect in *crs1* mutants very likely reflects a direct role for CRS1 in *atpF* splicing.

CRS1 is unrelated to previously described factors that facilitate group II intron splicing

The best studied class of group II intron splicing factor is the maturase family, a group of related proteins encoded within a subset of group II introns (reviewed by Lambowitz et al., 1999). Biochemical studies of the *Lactococcus lactis* LtrA maturase revealed that it binds to its own coding region and, in so doing, facilitates the splicing of its host intron (Wank et al., 1999). Thus, maturase activity may have evolved as a means to minimize the impact of maturase gene insertions on their host introns by preventing a disruption in intron folding that would otherwise arise from the additional RNA segment. This origin as a "selfish" passenger is conceptually distinct from the recruitment of factors to nucleate, stabilize, or participate in the catalytic core of group II introns. Mutations in nuclear genes that disrupt the splicing of organellar introns may reveal factors of these latter types. The yeast protein MSS116, which influences the splicing of group I and group II introns in mitochondria, is an RNA helicase and may facilitate splicing by resolving misfolded introns (Niemer et al., 1995). Genetic screens in *Chlamydomonas reinhardtii* revealed 14 nuclear genes that are required for the *trans*-splicing of one or both of the split group II introns in the chloroplast *psaA* gene (Goldschmidt-Clermont et al., 1990). The molecular cloning of two of these genes has been reported: *Maa2* exhibits homology to pseudouridine synthases (Perron et al., 1999) whereas *Raa3* is a novel protein that is found in a complex containing a segment of its target intron (Rivier et al., 2001). Mutations in the yeast nuclear gene *MRS2* disrupt the splicing of mitochondrial group II introns (Wiesenberger et al., 1992), but MRS2 appears to influence

splicing indirectly by altering the mitochondrial Mg^{2+} concentration (Bui et al., 1999). Finally, genetic screens in maize identified two nucleus-encoded factors required for group II intron splicing in chloroplasts, CRS1 and CRS2 (Jenkins et al., 1997). CRS2 is homologous to peptidyl-tRNA hydrolase enzymes and is found in a ribonucleoprotein complex in the chloroplast stroma (Jenkins & Barkan, 2001). Results presented here show that CRS1 is a novel group II intron splicing factor, highly basic in nature and lacking similarity to proteins of known function.

CRS1 is the founding member of a gene family in plants that arose by duplication of an ancient domain

CRS1 is a member of a predicted plant gene family represented by 16 members in *Arabidopsis*. Members of the CRS1 family contain between one and four degenerate copies of a 10-kDa basic domain. This domain appears to have been derived from an ancestral gene that predates the evolution of plants and algae. It is represented by a free-standing open reading frame in seven of the eight available archaeal genome sequences, including representatives from each of the major archaeal lineages, indicating that this gene was present in the progenitor of extant archaea. It is also represented in two major eubacterial lineages, the purple bacteria and the gram positive bacteria. Related genes have not been detected in fungal or animal genomes.

Among the conserved motifs within this domain is the sequence lGrxG (Fig. 5), which matches a conserved feature of the KH RNA binding domain (Siomi et al., 1993) that contacts RNA (Lewis et al., 2000). Although, the predicted secondary structure of the "CRS1 domain" (data not shown) is inconsistent with that of the canonical KH domain (Lewis et al., 2000; Grishin, 2001), it is nonetheless plausible that the CRS1 and KH domains are related in structure and function. Elucidation of the function and structure of the ancestral domain should bear on the biochemical role of members of the CRS1 family in plants.

The splicing of the *atpF* intron involves multiple factors

Maize and barley mutants lacking plastid ribosomes fail to splice the *atpF* intron and all other plastid introns in subgroup IIA (Hess et al., 1994; Huebschmann et al., 1996; Jenkins et al., 1997; Vogel et al., 1999). This has led to the idea that a chloroplast gene product functions in the splicing of all chloroplast group IIA introns, but other explanations remain plausible. We addressed one alternative: that *crs1* is down-regulated in cells lacking plastid ribosomes, resulting in the failure to splice the *atpF* intron. In fact, *crs1* mRNA does accumulate to reduced levels in *iojap* mutants lacking plastid ribosomes, and this may contribute to their *atpF* splicing defect. However, the magnitude of this decrease seems unlikely to account for the complete absence of *atpF* splicing in *iojap* plastids, and the involvement of a chloroplast gene product in *atpF* splicing remains a possibility. This splicing function may reside in MatK, a maturase-like protein encoded in an open reading frame within the plastid *trnK* intron (Neuhaus & Link, 1987; Liere & Link, 1995).

The participation of multiple factors in *atpF* splicing is now further supported by our finding that CRS1 is bound in a large stromal complex. This complex, at >600 kDa, is significantly larger than the combined size of CRS1 (~80 kDa) and the *atpF* intron RNA (~270 kDa) with which it appears to be associated. Possibly, MatK represents a core component in a spliceosome-like particle specific for group IIA introns in the chloroplast, and different members of the CRS1 family serve to target the complex to different group IIA introns.

Multiple functions for *crs1*

Although the original mutant allele, *crs1-1*, conditions a relatively specific loss of the chloroplast ATP synthase, a new allele, *crs1-2*, conditions a more severe chlorophyll deficiency and a more global loss of chloroplast-encoded proteins. These differences reflect the fact that *crs1-2* is a tighter allele due to the presence of a *Mu* insertion within the open reading frame (Fig. 1). The results of chloroplast polysome analysis (Fig. 11) indicate that *crs1* influences the chloroplast translation process or the biogenesis of the translation machinery. Previous analyses of other mutants lacking the ATP synthase (Jenkins et al., 1997) showed that a defect in chloroplast translation is not simply a consequence of an ATP synthase deficiency. The parsimonious possibility that *crs1* functions in the splicing of a chloroplast tRNA or ribosomal protein mRNA was eliminated by showing that the splicing of all such transcripts is normal in *crs1-2* mutants. Thus, the *crs1* gene appears to be bifunctional, participating in both *atpF* splicing and chloroplast translation. This is reminiscent of previous findings with proteins that function in concert with autocatalytic introns. CYT18 in *Neurospora crassa* and NAM2 in *Saccharomyces cerevisiae* are group I intron splicing factors that also function as tRNA synthetases (Li et al., 1996; Lambowitz et al., 1999; Rho & Martinis, 2000). The chloroplast group II intron splicing factors CRS2 and MAA2 evolved from a peptidyl-tRNA hydrolase and a pseudouridine synthase, respectively (Perron et al., 1999; Jenkins & Barkan, 2001). The translation defect conditioned by the *crs1-2* allele and the evolutionary relationship between CRS1 and an ancient conserved domain suggest that CRS1 may likewise have evolved from a component of the translation machinery.

Of possible relevance to the bifunctionality of *crs1* is the fact that two *crs1* mRNA forms exist, the products of alternative splicing. The predominant mRNA form encodes a protein of ~80 kDa that localizes to the chloroplast stroma. This 80-kDa CRS1 cosediments with *atpF* intron but not with ribosomes, implicating it in splicing. Although the predicted product of the minor mRNA form (~43 kDa) has not been detected, it remains possible that it plays a different role, perhaps functioning in translation. The predicted 43-kDa product lacks $1\frac{1}{2}$ copies of the 10-kDa domain that is found in three copies in the 80-kDa CRS1 form (see Fig. 4). The fact that this domain is encoded as a free-standing open reading frame in prokaryotic genomes indicates that a single copy is sufficient for its ancestral function. The predicted 43-kDa CRS1 may therefore have a function that is more closely akin to that of the ancestral domain than is the group II splicing function of the 80 kDa form.

Previously it was observed that *crs1* mutants accumulate increased levels of certain tRNA precursors, leading to the suggestion that *crs1* may function in both tRNA processing and *atpF* splicing (Vogel et al., 1999). However, the significance of those results is unclear because we have observed similar tRNA precursor accumulation in several unrelated mutants with global plastid translation defects, and in plants that had been treated with inhibitors of plastid translation (B. Till and A. Barkan, unpubl. results). Thus, it is possible that the alteration in tRNA metabolism is a consequence rather than the cause of the global translation defect in *crs1-2* mutants. Further experiments will be required to resolve this issue.

Biochemical characterization of CRS1 should reveal the mechanism by which it activates the splicing of the *atpF* intron, and does so with specificity. The fungal proteins CYT18 and CBP2 facilitate the splicing of mitochondrial group I introns by stabilizing an on-pathway folding intermediate or by stabilizing the fully assembled intron (reviewed by Lambowitz et al., 1999). CRS1 may function analogously, or it may function as an RNA chaperone to resolve misfolded intron RNAs and increase the yield of catalytically active intron (reviewed by Herschlag, 1995). Given that many members of the CRS1 family are predicted to be localized to mitochondria or chloroplasts, each of which harbor multiple group II introns, it is possible that other members of the CRS1 family may also function in group II intron splicing.

MATERIALS AND METHODS

Plant material and genetic analysis

Seedlings used for protein, RNA, and DNA extraction were grown in a growth chamber (16-h days at 28°C, 400 μE m^{-2} s^{-1}, and 8-h nights at 24 °C). To test for complementation of *crs1-2* and *crs1-1*, nine crosses were made between *crs1-1*/+ and *crs1-2*/+ plants. Each cross yielded ~$\frac{1}{4}$ chlorophyll-deficient mutants that lacked spliced *atpF* mRNA, indicating a failure to complement. The *crs1* locus was mapped to chromosome 1L by crossing *crs1-1*/+ plants to BA translocation stocks.

Nucleic acid extraction and analysis

RNA was extracted with TRIzol reagent (Gibco BRL) and Poly $(A)^+$ RNA was isolated using Oligo(dT) cellulose (Promega) according to manufacturer's instructions. Seedling DNA was extracted as previously described (Voelker et al., 1997). Genomic southern blots were prepared and probed with digoxigenin-labeled *Mu* probes as previously described (Voelker et al., 1997). Radiolabeled DNA probes were generated by priming with random hexamers. RNA gel blot and RNAse-protection assays were performed as previously described (Barkan et al., 1994; Jenkins et al., 1997). The *atpF* exon probe, *petB* intron probe, *atpF* intron probe, *ndhB* intron probe, and 16S rRNA probes for RNA gel blots, as well as the *rps12* intron 1, *rps12* intron 2, *rpl2*, *rpl16*, *rps16*, and *trnK* probes for RNAse protection assays were described previously (Barkan, 1993; Jenkins et al., 1997; Jenkins & Barkan, 2001).

Molecular cloning methods

To clone the *MuDR* containing fragment linked to *crs1*, 10 μg of DNA from a homozygous *crs1-1* mutant was digested with 30 units of *Bgl*II (New England Biolabs) for 16 h at 37 °C and fractionated on a 0.8% agarose gel. A gel slice containing DNA fragments of 4.4 to 4.6 kb was excised and the DNA purified. Of this DNA, 100 ng were ligated into 1 μg of Zap Express *Bam*HI phage arms that had been treated with calf intestinal phosphatase (Stratagene). The DNA was packaged using the Gigapack III gold packaging extract (Stratagene) and used to infect XL1-Blue MRF′ cells. A total of 2×10^5 plaques were screened by probing lifts with a radiolabeled *MuDR* probe, leading to the identification of the *Bgl*II fragment depicted in Figure 1A (GenBank accession number AF290416). Genomic sequence further downstream was amplified by PCR using primers complementary to the cDNA sequence (5′-ACTTTGGGCCCTC GATTTGT-3′ and 5′-TGCACTGAGGAGCTTCAGTGTTAC-3′; see below for cDNA cloning). Comparison of the DNA sequence of this genomic segment with that of the cloned cDNA sequence revealed the two introns diagramed in Figure 1A.

The genomic sequence flanking the *MuDR* insertion (clone A in Fig. 1A) was amplified from the original genomic clone by PCR using a primer specific to the *Mu* terminal inverted repeat (5′-AGAGAAGCCAACGCCAWCGCCTCYATTTCGTC-3′) in conjunction with a vector primer (pBK-CMV, Stratagene) (5′-CACACAGGAAACAGCTATGAC-3′). The ~2.3-kb product was purified and used as a hybridization probe for genomic southern blots and for screening the cDNA library. Sequence upstream of the *MuDR* insertion was obtained by cloning a 1,200 bp *Eco*RI fragment containing the "upstream" portion of the same *MuDR* insertion and flanking genomic sequence, using analogous methods.

A maize leaf cDNA library prepared from the inbred line B73 (Fisk et al., 1999) was screened with clone A, yielding a partial cDNA (GenBank accession number AF290415). To map additional transcribed sequences, RNase-protection as-

says were performed. Probes corresponding to the "left" side of the *MuDR* insertion (see Fig. 1A) were not protected from RNase, indicating that little if any of these sequences were represented in mRNA (data not shown). Probes corresponding to the "right" side of the *MuDR* insertion were fully protected in the region labeled as exon 1 in Figure 1A. A 2.4-kb cDNA was then obtained by RT-PCR using the Titan 1-step RT-PCR kit (ROCHE) and 1 μg of poly (A)$^+$ leaf RNA (inbred line B73) as template, according to the manufacturer's protocol. The following primers were used: (5′-TAGATATCTC TCCCCACATGGCG-3′) and (5′-TTTGCCAGTGCCTGGTT AGATC-3′). The reaction profile was: 50 °C/30 min, 94 °C/ 4 min, 45 °C/2 min, 72 °C/1.5 min, followed by 30 cycles of 94 °C/45 s, 64 °C/45 s, 72 °C/1.5 min, and a final extension of 72 °C/5 min. The resulting cDNA (GenBank accession number AF290414) is near full length, as evidenced by the facts that it is similar in size to the *crs1* mRNA detected on RNA gel blots, and that RNase protection assays failed to detected transcribed sequence upstream of the *MuDR* insertion.

Reverse genetic screen for identification of the *crs1-2* allele

A library of *Mu*-induced nonphotosynthetic maize mutants was used as a reservoir from which to identify a second mutant allele of *crs1*. This library consisted of DNAs extracted from ~1,300 independently arising mutants, grouped into 69 pools. To identify individuals with a *Mu* insertion within the cloned region, pools were screened by PCR using one primer specific to the terminal inverted repeat of *Mu* transposons (5′-AGAGAAGCCAACGCCAWCGCCTCYATTTCG TC-3′) and one primer specific to *crs1* exon 1 (5′-GTG TGGACGGAATTCGGACTC-3′). PCR reactions (50 μL) contained 0.5% DMSO, PCR Buffer (50 Mm KCl, 10 mM Tris-HCl, pH 9, 0.1% Triton X-100, 1.5 mM $MgCl_2$ 2 mM dNTPs), Taq Polymerase, and 100 ng of DNA template, and were incubated as follows: 94 °C/4 min, followed by 35 cycles of 94 °C/45 s, 62 °C/1 min, 72 °C/2 min, and a final extension of 72 °C for 4 min. Products were analyzed by southern hybridization with a clone A probe (Fig. 1A). DNAs from individuals in pools that scored positive were then screened by PCR, yielding a single positive individual. The *Mu* insertion site in this individual was determined by DNA sequence analysis of the amplification product, revealing an insertion of a *Mu1* element in exon 1 (see Fig. 1). After complementation tests confirmed that this new mutation was allelic with *crs1-1*, this new allele was termed *crs1-2.*

Quantification of alternatively-spliced *crs1* mRNAs

Primer 2 diagramed in Figure 6 (5′-AAGTGAGTCAACTG CTTTCAGTCG-3′) was used to prime reverse transcription with 10 μg of total RNA as template. Dilutions of the leaf tip RNA sample were assayed to demonstrate linearity of the assay. Each reaction (20 μL) contained 100 ng of primer, 30 U of rRNasin ribonuclease inhibitor (Promega), 50 mM Tris-HCL (pH 8.3 at 25 °C), 75 mM KCl, 5 mM $MgCl_2$, 10 mM DTT, 0.5 mM dNTPs, and 200 U of M-MLV reverse transcriptase (Promega). Template RNA and primer were first heated for 3 min at 90 °C followed by chilling on ice for 2 min. rRNasin, buffer, and dNTPs were then added and reactions were incubated at 42 °C for 2 min prior to the addition of M-MLV (+RT samples) or an equal amount of water (−RT samples). After 1 h at 42 °C, template RNA was degraded by the addition of 2.5 U of RNase H (USB) and incubation for 20 min at 37 °C. Reverse transcription products were purified using the QIAquick PCR purification kit (Qiagen). PCRs were then performed using primer 1 (5′-ACTCCATATAGGCTGTGCCCT-3′) and primer 2 (sequence given above) diagramed in Figure 6. Reactions (50 μL) contained 2 μL of eluted cDNA in PCR buffer and were amplified under the following conditions: 94 °C/4 min, followed by 30 cycles of 94 °C/45 s, 62 °C/ 45 s, 72 °C/1 min, and a final extension of 72 °C/5 min. Positive controls for each spliced product were generated using the same PCR conditions with either 50 ng of the *crs1* cDNA recovered from the cDNA library ("alternatively" spliced) or 50 ng of the *crs1* cDNA obtained by RT-PCR ("fully" spliced). Twenty nanograms of each control and 15 μL of each RT-PCR product were fractionated on an agarose gel and analyzed by southern hybridization by probing with a *crs1* cDNA fragment.

Protein extraction, leaf cell fractionation, and immunoblot analysis

Methods for the extraction of total leaf protein, SDS-PAGE, and immunoblot analysis have been described previously (Barkan, 1998). Intact chloroplasts were purified from the leaves of 10-day-old seedlings using Percoll step gradients (Barkan, 1998), and fractionated into stromal, thylakoid, and envelope fractions as described (Fisk et al., 1999).

Sucrose gradient analysis

Stromal samples were prepared and analyzed by sucrose gradient sedimentation as described (Jenkins & Barkan, 2001). To test the effect of RNase on the CRS1 complex, 2 μg RNase A (Sigma) were added to 2.5 mg of stromal protein extract in a volume of 250 μL and incubated for 15 min at room temperature. This material was then applied to a 10–40% sucrose gradient and centrifuged at 48,000 rpm for 190 min in an SW55.1 rotor. RNA was extracted from 60 μL of each fraction in 0.75 mL TRIzol Reagent (Gibco BRL).

Antisera

A recombinant CRS1 fragment (amino acids 213–541) was generated by ligating a portion of the *crs1* cDNA into the pQE-30 vector (Qiagen), yielding a translation product with an N terminal 6× histidine tag. The fusion protein was purified on a nickel column and injected into rabbits for the production of polyclonal antisera. Antisera were generated by the University of Oregon antibody facility. The sera were affinity purified against the same antigen.

Antibody to CRP1 was described in Fisk et al. (1999), antibody to AtpA in McCormac & Barkan (1999), and antibodies to RbcL, PsbA, PsaD, PetD, and OE33 were described by Voelker & Barkan (1995). IM35 antibody was generously provided by Danny Schnell (Rutgers University), MDH antibody was generously provided by Kathy Newton (University of Missouri), and PEPcase antibody was generously provided by W. Taylor (CSIRO, Australia).

NOTE ADDED IN PROOF

Anti-CRS1 antiserum immunoprecipitates atpF intron RNA from chloroplast extracts, but does not immunoprecipitate several other chloroplast group II introns. This confirms that CRS1 is bound specifically to atpF intron RNA in vivo.

ACKNOWLEDGMENTS

The authors are indebted to Dianna Fisk and Bethany Jenkins for their generous donation of chloroplast and sucrose gradient fractions, and to Laura Roy, Susan Belcher, and Dennis McCormac who generated the mutant DNA library used in the reverse genetic screen. We are grateful to Bethany Jenkins, Gerry Ostheimer, Sebastian Klaus, and Dennis McCormac for useful discussions and to Kenny Watkins and Bethany Jenkins for providing comments on the manuscript. Macie Walker and Susan Belcher provided expert technical assistance. This work was supported by grant MCB-9904666 from the National Science Foundation.

Received March 28, 2001; returned for revision
April 19, 2001; revised manuscript received
May 25, 2001

REFERENCES

Barkan A. 1989. Tissue-dependent plastid RNA splicing in maize: Transcripts from four plastid genes are predominantly unspliced in leaf meristems and roots. *Plant Cell 1*:437–445.

Barkan A. 1993. Nuclear mutants of maize with defects in chloroplast polysome assembly have altered RNA metabolism. *Plant Cell 5*:389–402.

Barkan A. 1998. Approaches to investigating nuclear genes that function in chloroplast biogenesis in land plants. *Methods Enzymol 297*:38–57.

Barkan A, Voelker R, Mendel-Hartvig J, Johnson D, Walker M. 1995. Genetic analysis of chloroplast biogenesis in higher plants. *Physiologia Plantarum 93*:163–170.

Barkan A, Walker M, Nolasco M, Johnson D. 1994. A nuclear mutation in maize blocks the processing and translation of several chloroplast mRNAs and provides evidence for the differential translation of alternative mRNA forms. *EMBO J 13*:3170–3181.

Bennetzen JL. 1996. The Mutator transposable element system of maize. *Curr Top Microbiol Immunol 204*:195–229.

Bui D, Gregan J, Jarosch E, Ragnini A, Schweyen R. 1999. The bacterial magnesium transporter CorA can functionally substitute for its putative homologue Mrs2p in the yeast inner mitochondrial membrane. *J Biol Chem 274*:20438–20443.

Emanuelsson O, Nielsen H, Brunak S, Heijne Gv. 2000. Predicting subcellular localization of proteins based on their N-terminal amino acid sequence. *J Mol Biol 300*:1005–1016.

Fisk DG, Walker MB, Barkan A. 1999. Molecular cloning of the maize gene *crp1* reveals similarity between regulators of mitochondrial and chloroplast gene expression. *EMBO J 18*:2621–2630.

Goldschmidt-Clermont M, Girard-Bascou J, Choquet Y, Rochaix J-D. 1990. *Trans*-splicing mutants of *Chlamydomonas reinhardtii. Mol Gen Genet 223*:417–425.

Grishin N. 2001. KH domain: One motif, two folds. *Nucleic Acids Res 29*:638–643.

Herschlag D. 1995. RNA chaperones and the RNA folding problem. *J Biol Chem 270*:20871–20874.

Hess WR, Hoch B, Zeltz P, Huebschmann T, Koessel H, Boerner T. 1994. Inefficient *rpl2* splicing in barley mutants with ribosome-deficient plastids. *Plant Cell 6*:1455–1465.

Huebschmann T, Hess WR, Boerner T. 1996. Impaired splicing of the rps12 transcript in ribosome-deficient plastids. *Plant Mol Biol 30*:109–123.

Jenkins B, Barkan A. 2001. Recruitment of a peptidyl-tRNA hydrolase as a facilitator of group II intron splicing in chloroplasts. *EMBO J 20*:872–879.

Jenkins BD, Kulhanek DJ, Barkan A. 1997. Nuclear mutations that block group II RNA splicing in maize chloroplasts reveal several intron classes with distinct requirements for splicing factors. *Plant Cell 9*:283–296.

Lambowitz A, Caprara M, Zimmerly S, Perlman P. 1999. In: Gesteland RF, Cech T, Atkins J, eds., *Group I and group II ribozymes as RNPs: Clues to the past and guides to the future*. Cold Spring Harbor, New York: Cold Spring Harbor Laboratory Press. pp 451–485.

Lewis H, Musunuru K, Jensen K, Edo C, Chen H, Darnell R, Burley S. 2000. Sequence-specific RNA binding by a nova aKH domain: Implications for paraneoplastic disease and the fragile X syndrome. *Cell 100*:323–332.

Li G-Y, Becam A-M, Slonimski P, Herbert C. 1996. In vitro mutagenesis of the mitochondrial leucyl-tRNA synthetase of *Saccharomyces cerevisiae* shows that the suppressor activity of the mutant proteins is related to the splicing function of the wild type protein. *Mol Gen Genet 252*:667–675.

Liere K, Link G. 1995. RNA-binding activity of the *matK* protein encoded by the chloroplast *trnk* intron from mustard. *Nucleic Acids Res 23*:917–921.

McCormac D, Barkan A. 1999. A nuclear gene in maize required for the translation of the chloroplast *atpB/E* mRNA. *Plant Cell 11*:1709–1716.

Michel F, Umesono K, Ozeki H. 1989. Comparative and functional anatomy of group II catalytic introns—A review. *Gene 82*:5–30.

Neuhaus H, Link G. 1987. The chloroplast tRNA(Lys)(UUU) gene from mustard (*Sinapis alba*) contains a class II intron potentially encoding for a maturase-related polypeptide. *Curr Genet 11*:251–257.

Niemer I, Schmelzer C, Boerner GV. 1995. Overexpression of DEAD box protein pMSS116 promotes ATP-dependent splicing of a yeast group II intron in vitro. *Nucleic Acids Res 23*:2966–2972.

Perron K, Goldschmidt-Clermont M, Rochaix J-D. 1999. A factor related to pseudouridine synthases is required for chloroplast group II intron *trans*-splicing in *Chlamydomonas reinhardtii. EMBO J 18*:6481–6490.

Rho S, Martinis S. 2000. The bI4 group I intron binds directly to both its protein splicing partners, a tRNA synthetase and maturase, to facilitate RNA splicing activity. *RNA 6*:1882–1894.

Rivier C, Goldschmidt-Clermont M, Rochaix JD. 2001. Identification of an RNA–protein complex involved in chloroplast group II intron *trans*-splicing in *Chlamydomonas reinhardtii. EMBO J 20*:1765–1773.

Siomi H, Matunis M, Michael W, Dreyfuss G. 1993. The pre-mRNA binding K protein contains a novel evolutionarily conserved motif. *Nucleic Acids Res 21*:1193–1198.

Surpin M, Chory J. 1997. The coordination of nuclear and organellar genome expression in eucaryotic cells. *Essays Biochem 32*:113–125.

Voelker R, Barkan A. 1995. Two nuclear mutations disrupt distinct pathways for targeting proteins to the chloroplast thylakoid. *EMBO J 14*:3905–3914.

Voelker R, Mendel-Hartvig J, Barkan A. 1997. Transposon-disruption of a maize nuclear gene, *tha1*, encoding a chloroplast SecA homolog: In vivo role of cp-SecA in thylakoid protein targeting. *Genetics 145*:467–478.

Vogel J, Boerner T, Hess W. 1999. Comparative analysis of splicing of the complete set of chloroplast group II introns in three higher plant mutants. *Nucleic Acids Res 27*:3866–3874.

Walbot V, Coe EH. 1979. Nuclear gene *iojap* conditions a programmed change to ribosome-less plastids in *Zea mays*. *Proc Natl Acad Sci USA 76*:2760–2764.

Wank H, SanFilippo J, Singh R, Matsuura M, Lambowitz A. 1999. A reverse transcriptase/maturase promotes splicing by binding at its own coding segment in a group II intron RNA. *Mol Cell 4*:239–250.

Wiesenberger G, Waldherr M, Schweyen R. 1992. The nuclear gene MRS2 is essential for the excision of group II introns from yeast mitochondrial transcripts in vivo. *J Biol Chem 267*:6963–6969.